Sensors & Transducers, Vol. 28, Special Issue, April-May 2018, pp. 43-53

www.sensorsportal.com

Sensors & Transducers

Published by IFSA Publishing, S. L., 2018
http://www.sensorsportal.com

Tailoring the Preparation of Fluorescent Molecularly Imprinted Polymers (MIPs) Toward the Detection of Chemical Warfare Agents

[1, 2] Dahlia C. Apodaca, [1] Nicholas Turner, [1] Michael Bowyer, [1] Clovia Z. Holdsworth and [1] Adam McCluskey

[1] Discipline of Chemistry, School of Environmental and Life Sciences, University of Newcastle, Callaghan, NSW 2308 Australia

[2] School of Chemical, Biological and Materials Engineering and Sciences, MAPUA University, Intramuros, Manila, Philippines 1002

[1] Tel.: +639178035868

E-mail: dcapodaca@yahoo.com

Received: 28 March 2018 /Accepted: 28 May 2018 /Published: 31 May 2018

Abstract: The efficiency of the molecular imprinting technology to detect a specific target analyte rests on the success of the optimization techniques employed prior to fabrication/polymerization. In this work, the influence of the nature and amount of crosslinker as well as the template-monomer ratio on the fluorescence intensity of two fluorescent polymers, 7-hydroxy-4-methylcoumarin acrylate (HMC) and 2,6-bis-acrylamidopyridine (BAP) were investigated. Target analytes were 1,4-dinitrotoluene (DNT, precursor in the preparation of TNT) and trinitrotoluene (TNT) and ricinine, an analogue of ricin. Ethylene glycol dimethacrylate (EGDMA), trimethylolpropane trimethacrylate (TRIM) and divinyl benzene (DV55), were used as crosslinkers. It was observed that both ricinine and TNT tend to quench the fluorescence emission of HMC monomer, which is deemed useful as a mode of signal transduction to indicate the binding of these templates with the MIP sensor. Further characterization showed that HMC-based MIP prepared using DV55 as crosslinker gave the most pronounced quenching effect. On the other hand, MIP prepared using EGDMA as cross linker, was found to fluoresce strongly, with the following order of relative intensities: EGDMA > TRIM > DV55. Meanwhile, in contrast with the observations in HMC-MIP, there was an enhancement on the fluorescent signal generated by BAP-MIP in the presence of template molecules. In addition, changing the molar ratio of EGDMA in MIP and NIP prepared from BAP functional monomer also could influence the fluorescence intensities. Results suggest that both MIP and NIP prepared using a molar ratio of 1:4:10 (DNT:BAP:EGDMA) generated the highest fluorescence intensity as compared to samples with ratio 1:4:20 and 1:4:30 (DNT:BAP:EGDMA).

Keywords: Fluorescence, Molecularly imprinted polymer, Warfare agents, Sensor, Quenching.

1. Introduction

Molecular imprinting is a technique used for the preparation of polymeric materials intended for molecular recognition. This method is based on the preparation of a highly cross linked polymer around a template, which is the target analyte, in the presence of a suitable functional monomer [1]. The process involves interactive preorganization of functional monomers such that specific chemical interactions

occur between functional monomers and "print" molecules, followed by polymerization in the presence of a large excess of cross linking agents. The resulting polymer contains specific binding sites that recognize the print molecule thus exhibiting a high selectivity for rebinding the print with which it was prepared [2].

One of the significant applications of molecularly imprinted polymer is in the preparation of sensors. The biomimetic properties of molecularly imprinted polymers render them attractive as recognition molecules in chemical sensors [3]. Acts of biological terrorism (bioterrorism) have been the driving force in the screening of various receptor molecules for detecting potential biological toxins. Recent reports about terrorist actions are alarming and the detection of biological and chemical warfare agents has become one of the highest research priorities in the fields of security and public health.

Ricin is a biological weapon that may be used for bioterrorist purposes because of its easy production, wide availability and the lack of specific treatment of ricin poisoning [3]. Ricin is highly toxic lectin originating from the castor bean plant *Ricinus communis*, and is composed of a catalytic chain A linked to a lectinic B chain by a disulfide bridge. The B chain mediates the cellular binding and entry of the A chain which possesses the N-glycosidase activity and inhibits protein synthesis. The US Chemical Warfare Services studied ricin as a potential weapon during World War I while the British Military, during the World War II, developed a ricin bomb. Around 1978, bizarre assassinations involving a ricin-spiked umbrella were reported [4]. The toxicity of ricin measured in terms of the LD50 in mice is on the order of 2 μg/kg body weight after intraperitoneal injection and between 3 and 30 μg/kg after inhalation or oral absorption [5].

Structure-based bioassays are the main approaches for detection of toxins. Structure-based methods, such as immunoassays, have been widely applied for the identification and quantification of ricin; however, these methods cannot address the needs for detection of unanticipated threats. ELISA and immuno-polymerase chain reaction assay offer good prospects for the analysis and quantification of ricin with detection limits between 0.1 and 80 ng/mL and 10 fg/mL, respectively. Alternative method for the detection of ricin involves the use of glycosphingolipids [6]. Investigation of the interaction of mannose-substituted poly (para phenyl-eneethynylene) (mPPE) with a lectin, Concanavalin A has also been reported to model ricin detection [7]. Current methods for unambiguous identification of ricin include molecular weight determination by MALDI-MS and in vivo toxicity testing [8].

Since ricin is listed in Schedule 1 of the Chemical Weapons Convention, handling of ricin is subject to inspection and control measures, a recent study has proposed for the alkaloid ricinine as an indirect indicator of the presence of ricin in crude plant extracts, urine from potentially exposed persons or both [9]. Ricinine is an alkaloid (3-cyano-4-methoxy-N-methyl-2-pyridone) that shares a common plant source with ricin, and its presence in urine infers ricin exposure. Ricinine is present in crude preparations of ricin, and it can be found in human urine after a lethal exposure to ricin [9]. Thus sensing ricinine is proportionate to sensing ricin.

Ricinine is a neutral alkaloid isolated which induces seizures when administered to mice at doses higher than 20 mg/kg. Animals presenting seizures showed a marked preconvulsive phase followed by short duration hind limb myoclonus, respiratory spasms and death [10, 11]. The structure of ricinine is given in Fig. 1.

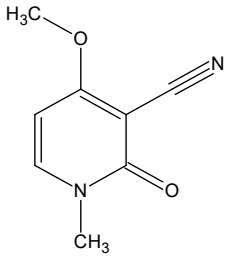

Fig. 1. Structure of N-methyl-3-cyano-4-methoxy-2-pyridone, commonly known as ricinine.

On the other hand, trinitrotoluene is a powerful explosive compounds which not only posed security threat but can also cause pancytopenia, a disease associated with blood-forming tissues in humans [12]. As such, sensor devices capable of detecting and monitoring TNT and its precursor, DNT is equally important. Fig. 2 shows the chemical structures of TNT and its precursor, DNT.

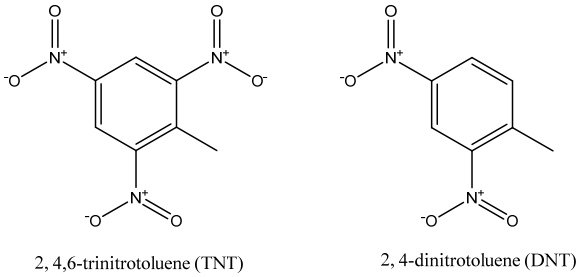

Fig. 2. Chemical structures of TNT and DNT.

Fluorescent monomers when incorporated in a molecularly imprinted polymer (MIP) formulation offer high sensitivity and high selectivity by monitoring their fluorescent signal upon binding with the target analyte [13]. Because of this, fluorescent MIP sensors have become a powerful alternative MIP assay format for the detection of various analytes. Among those fluorescent monomers which have been recently used for molecular imprinting applications were naphthalimide-based derivatives [14 a, b],

dansyl methacrylate [15] and boronic acid [13]. In the past, Kubo, *et al*. [16] reported the use of the fluorescent monomer 2,6-bis(acrylamido)pyridine for the imprinting of cyclobarbital. Previously, they have reported on imprinted polymers using 2,6-bis(acrylamido)pyridine as a functional monomer that was capable of forming multiple hydrogen bonding with barbiturates and 5-fluorouracil. Since 2,6-bis(acrylamido)pyridine shows strong fluorescence, they also investigated whether or not 2,6-bis(acrylamido)pyridine works as a signaling monomer for molecular imprinting of cyclobarbital. Results suggest that there was an enhancement in the fluorescence intensity of 2,6-bis(acrylamido)pyridine upon binding with cyclobarbital.

On the other hand, Thanh, *et al*. [17] prepared imprinted polymer cavities selective for cGMP using the easily-obtained fluorescent functional monomer, 2-acrylamidopyridine. Results show that the polymer was found to display high affinity and selectivity for aqueous cGMP over GMP and cAMP.

Meanwhile, Karube I., *et al*. [18], developed a fluorescence sensing system based on a combination of an MIP and HPLC for the detection of the steroid hormone β-estradiol. Two approaches were explored: (a) direct measurement of the β-estradiol fluorescence; (b) a method based on the competitive displacement by the analyte of a fluorescent compound from specific binding sites in the imprinted polymer.

A novel design for template-selective recognition sites in polymers prepared by molecular imprinting was presented by Wandelt B., *et al*. [19]. Molecular imprints were prepared against cAMP that contain a fluorescent dye, *trans*-4-[p-(N,N-dimethy-lamino)styryl]-N-vinylbenzylpyridinium chloride, as an integral part of the recognition cavity, thus serving as both the recognition element and the measuring element for the fluorescence detection of cAMP in aqueous media. This fluorescent molecularly imprinted polymer displays a quenching of fluorescence in the presence of aqueous cAMP, whereas almost no effect is observed in the presence of the structurally similar molecule, cGMP.

A paper presented by Mosbach K., *et al*. [20] discussed the use of a fiber-optic sensing device, which manifested enantiospecificity for a fluorescence labeled amino acid (dansyl-L-phenylalanine) based on molecularly imprinted polymers (MIPs). The polymers' used in their model system exhibited strong binding to the imprint species, dansylphenylalanine.

In view thereof, monitoring of fluorescent signal from MIP systems, be it quenching or enhancement, often requires systematic and rational design.[21] For instance, functional monomers for fluorescent MIP applications are not widely available and may have to be synthesized. These functional monomers may significantly alter the conformation of the template after polymerization and could result to changes in its fluorescence response. [22] It is therefore necessary to carefully design the fabrication of MIP to include 1) Establishing the molar ratio between the template and monomer, suffice to give the optimum template-monomer (T:M) interactions; 2) Determining the extent of crosslinking, and 3) Optimizing the type and amount of crosslinkers, and many others, to ensure successful imprinting. There has been limited number of literatures indicating the use of fluorescence as a detection scheme in the preparation of MIPs for the detection of ricinine, DNT and other chemical warfare agents. Molecular modeling using Spartan® software in tandem with NMR titration studies were performed to determine which T:M ratio would be favorable for polymerization as evidenced by the calculated change in stabilization energy. Therefore this study explored the development of a chemical sensor based on fluorescent molecularly imprinted polymer as a tool for the sensitive detection of ricinine, TNT and DNT. Specifically, efforts were directed to optimize the fluorescent MIP formulation. This study has investigated the influence of: 1) Crosslinkers such as divinyl benzene (DVB), ethylene glycol dimethacrylate (EGDMA) and trimethylolpropane trimethacrylate (TRIM) on the fluorescent signals of BAP and HMC; 2) Varying molar ratios of crosslinkers on the fluorescence of 2, -(bis)-acrylamidopyridine (BAP) and 7-hydroxy-4-methylcoumarin acrylate (HMC). The resulting imprinted polymers are assumed to possess structural rigidity brought about by the interaction of BAP and HMC with the target analyte, allowing the MIP to respond via changing fluorescence signal intensity upon binding with ricinine, DNT, TNT and other chemical warfare agents.

This study highlights the important application of molecular imprinting in the formulation of polymeric receptor for the detection of chemical warfare agents. Thus, due to this concern, a study must be carried out to address the need for a cost-effective and robust detection system for these compounds using sensitive fluorescent signaling MIPs.

2. Experimental

Chemicals. All reagents and solvents employed for this study were analytical grade and were purchased from a variety of commercial sources. Azobisisobutyronitrile (AIBN) was recrystallized from acetone and was dried under vacuum at room temperature. Ethyleneglycoldimethacrylate (EGDMA, Sigma-Aldrich) was either distilled under reduced pressure before use or washed with 1 M NaCl three times to remove all stabilizers. After recovery of the organic layer, it was dried with anhydrous magnesium sulfate and filtered. Fluorescent monomers will be prepared according to the following series of procedures as adopted from published literatures [23, 24] 2,6-diaminopyridine (2,6-DAP) was used after recrystallization from benzene (mp 118 ^{o}C). Figure 3 gives the chemical reaction associated with the synthesis of BAP and HMC fluorescent monomers. Triethylamine (12.1 g,

120 mmol) and 2, 6-diaminopyridine (5.46 g, 50 mmol) was dissolved in 150 ml of chloroform and chilled at 0 ºC. Acryloyl chloride (10.9 g, 120 mmol) was gradually added and the reaction mixture was stirred for 12 h. The solvent was removed in vacuo and the precipitate was subsequently dissolved in 200 ml of methanol; 100 ml of the methanol solution was then gradually added to 800 ml of distilled water with stirring. Filtration of the mixture yielded the functional monomer, 2,6-(bis)acrylamidopyridine (1.37 g, 35 %), the structure of which was identified using a ^{1}H-NMR spectrometer.

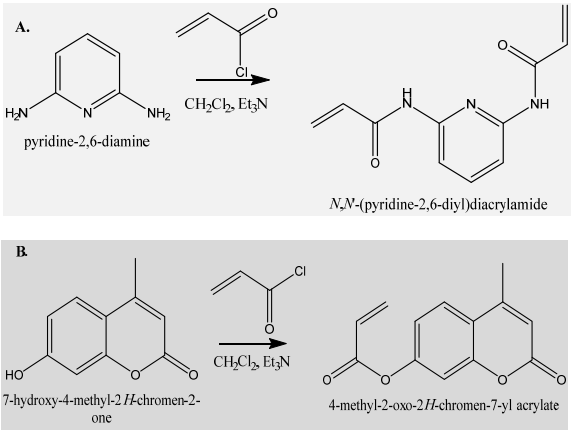

Fig. 3. Chemical reactions showing the synthesis of a) 2,6(bis)-acrylamidopyridine and b) hydroxyl methyl coumarin.

Molecular modeling. Modeling studies were performed to determine the extent of interaction that exists between the monomers and the templates. The extent of such interaction is quantified through calculated free energy changes exerted by the interacting molecules. Specifically, equilibrium geometry calculations at the ground state using the semi-empirical method, AM1 was carried out using Spartan 04 (Wavefunction, Inc., California, USA). The energy of interaction of the template-monomer complex was obtained from calculated enthalpies of formation (stabilization energy).

NMR Experiments. NMR spectra were recorded on a ^{1}H 300 MHz Bruker Avance instrument in deuterated DMSO-d_6. NMR titration was performed by adding increasing molar equivalents of the monomers to the templates (5:1, 4:1, 3:1, 2:1 and 1:1), keeping the final concentration and volume of solution the same in all the solutions used in titration experiments.

Preparation of fluorescent MIPs. The fluorescent MIPS were prepared in template/monomer molar ratio of 1:4. These were then combined with AIBN as initiator and crosslinkers in 2 mL of distilled dimethylformamide (DMF) as porogen. The mixture was sonicated for at least 5 minutes to ensure complete dissolution of all the components. The reaction mixtures were then degassed by purging with N_2 gas, sealed with Parafilm® and polymerized at 60 ºC for 12 hours, after which the bulk polymers were washed in methanol, ground to uniform size (< 38 μm), and then wet sieved. Fluorescent monomers were then transferred to paper thimble for subsequent template removal. Template removal was done via Soxhlet extraction for 18 hours using methanol:acetic acid (9:1, v/v) solvent system. The extraction process was monitored by FT-IR and was continued until no template peaks were evident. The non-imprinted polymers (NIP) served as control and were prepared and treated in similar manner.

Rebinding studies. The fluorescent MIPs were suspended in 2 mL of template solution in DMSO for the desired duration. The concentration of the solution before and after rebinding was determined by fluorescence measurement using Cary Eclipse spectrofluorometer. All analyses were conducted in two trials.

Scanning Electron Microscopy (SEM). SEM images were obtained using a Philips XL30 scanning electron microscope and Oxford ISIS EDS (1997) software.

3. Results and Discussion

3.1. Molecular Modeling Studies

Molecular modeling studies were performed using Spartan'04 (Wavefunction, USA) via semi empirical method (AM1) to locate the most favorable template-monomer clusters. Computational studies involved the following procedures: 1) evaluation of the energy of the initial structures drawn, called energy minimization. It may either be the template or the monomer units; 2) random translation and rotation of the second structure about the first structure; and 3) evaluation of the energy of the new system, in this case, the monomer-template complex. The extent of interaction (change in stabilization energy) energies for each T: M ratio, were calculated using the equation given below:

ΔE = E (template – monomer complex) - [E(template) + E(monomer)] [25].

It should be emphasized however, that the interactions were performed in vacuum, that is, the assumption was that there were no solvent molecules included in the calculations.

Both template and functional monomer possess functional groups capable of forming pre-polymerization complexes in solution similar to what is shown in Fig. 4.

As it is shown, the induce pre-association was attributable to noncovalent interactions such as hydrogen bond formation and possibly through π-π stacking. Table 1 summarizes the calculated enthalpies.

Results show that generally, 1:2 template:monomer (T:M) ratio yielded the large change in stabilization energy, that is, the most negative enthalpy. Exception noted was the predicted interactions between HMC and ricinine. A pronounced interaction was to be expected at 1:4 T:M ratio. At these predicted T:M ratios, there was no significant aggregation of functional monomers due to formation of hydrogen bonds between monomers.

Fig. 4. Spartan-generated figure illustrating pre-association of HMC monomer units with the template, TNT, (2:1 monomer:template ratio).

Table 1. Calculated Stabilization Energies for each template-monomer complex.

Template	Monomer	ΔStabilization Energy, kcal/mol	Complex T:M
TNT	HMC	-5.7	1:2
	BAP	-5.4	1:2
DNT	HMC	-1.9	1:2
	BAP	-4.0	1:2
Ricinine	HMC	-5.4	1:4
	BAP	-6.0	1:2

3.2. NMR Titration

To complement the results obtained from computational studies, NMR titration was performed to further investigate the interactions between the functional monomer and the template. In this technique, actual interaction was measured in solution, that is, each template were combined with varying ratios of functional monomer and were both dissolved in deuterated DMSO. The change in the chemical shift of both aromatic H and $–CH_3$ were monitored in the presence of different ratios of functional monomer. Changes in the chemical shifts may be attributed to the hydrogen bond formations which were also observed from modelling studies. [26] Downfield shift is expected in the case of hydrogen bond formation, implying the loss of electron density.

As shown in Fig. 5, HMC monomer gives distinct interactions toward TNT and ricinine as implied by the difference in the curves given by the plots. And that as the HMC monomer units was increased, the extent of interaction also tend to change. In the case of TNT template, the change in the chemical shift of both protons (aromatic and methyl) tends to decrease with increasing amount of HMC added. It was rationalized that the decrease could be attributed to increasing monomer-monomer interactions instead of favourable template-monomer interactions. Moreover, it was observed that the change in the chemical shift was pronounced with the 1:3 T:M cluster.

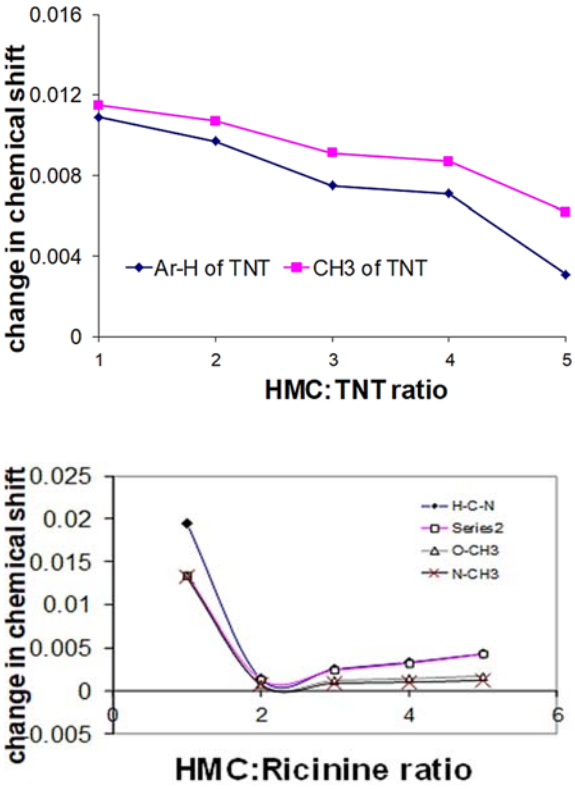

Fig. 5. Change in chemical shifts of protons of templates, TNT and ricinine, as a function of increasing amounts of HMC monomer.

On the other hand, a sharp decrease in the change in chemical shift was noted upon the interaction of HMC monomer with ricinine as template. The curve then gives a plateau at 1:3 T:M ratio suggesting that there were no significant interactions further taking place at increasing amount of HMC.

NMR titration plots further suggest that the interaction of HMC with TNT involved only one kind of complexation equilibrium as compared to the predicted interaction of HMC with ricinine. There were at least two inflection curves indicating two possible clustering (pre-association) mechanisms may be in place [25].

Computational studies aimed at establishing the interactions of HMC with TNT correlate well with the interactions obtained from NMR titration studies. Both suggest that the favorable T:M stoichiometry is

1:2. Meanwhile, in the case of ricinine, favorable interactions were noted using 1:2 (NMR titration) and 1:4 (computational modeling) T:M ratios.

3.3. Fluorescence Measurements

Fluorescence studies show that TNT tends to quench the fluorescence emission of HMC monomer. HMC yields emission intensity at λ_{em} = 391 nm (λ_{ex} = 345 nm) of ~115 nm, which significantly dropped in the presence of TNT. Such reduction in the emission intensity justifies the interactions of the HMC functional monomers with the template as predicted from modelling and NMR titration studies. In addition, further fluorescence studies suggest that both ricinine and TNT tend to quench the fluorescence signal of HMC monomer. This reduction in the fluorescence intensity in the presence of template can be used as a mode of signal transduction to indicate sensing of template by fluorescent MIPs. Moreover, it was found that TNT tends to quench the fluorescent signal to a large extent compared to ricinine. This could be due to the photoinduced electron transfer from the excited fluorescent MIP molecules to the analytes. TNT contains electron deficient nitroaromatic groups which facilitates such photoinduced electron transfer [27].

On another note, it was established that MIP-HMC, with and without TNT (after template removal), gave relatively lower emission intensity as compared with NIP-HMC which may imply differences in the structure brought about by relative rigidity in the MIP-HMC structure in the presence of template molecules. This observation further manifests the imprinting effect in which the MIP displays higher affinity toward the TNT template compared to NIP. The large extent of quenching can be equated to the binding of TNT to the MIP.

3.4. Synthesis of Fluorescent MIPs: Optimization

Rational design of fluorescent MIP systems for the detection of chemical warfare agents is highlighted in this study. This study investigated the influence of using different types and amounts of crosslinkers in the MIP formulation [28]. The addition of a crosslinker in the MIP formulation will provide the adequate rigidity and polymeric support that is necessary in keeping the cavities or binding sites on MIP structure intact and reliable during binding [29, 30]. This is to preclude the possibility that the fluorescent quenching may be due to nonspecific binding. That with the correct formulation, cavities or binding sites will be created on MIP structures, effectively giving distinguishable fluorescent signals especially upon detection of target analytes by MIP fluorescent sensor.

3.4.1. Effect of Varying Types and Amounts of Crosslinkers on HMC-MIP

Trimethylolpropane trimethacrylate (TRIM), divinyl benzene (DVB) and ethylene glycol dimethacrylate (EGDMA) were used as crosslinkers in the MIP formulation. Results shown in Figure 6, suggest that MIP prepared using EGDMA as cross linker, fluoresced strongly, with the following order of relative intensities: EGDMA > TRIM > DVB. EGDMA may have provided a relatively rigid polymeric network as compared to other MIP formulations containing different cross linker. It could be that the degree of crosslinking in the MIP structure was not as high as what was achieved with EGDMA. Further, it was noted that NIPs-HMC yielded relatively higher fluorescence intensities than MIPs-HMC, again signifying the influence of the presence of the template molecule on the MIP structure, resulting to pronounce quenching.

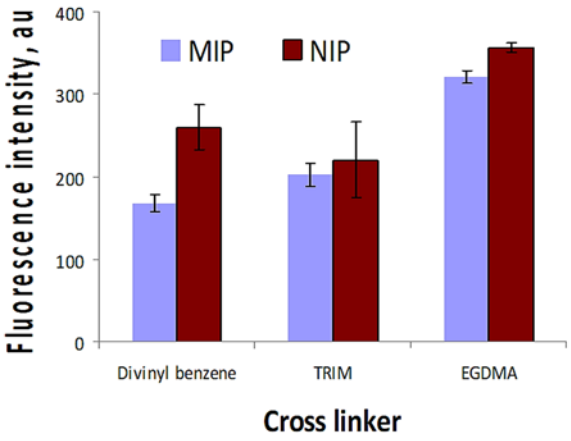

Fig. 6. Comparison of the fluorescent signals of MIPs and NIPs made from different kinds of crosslinkers and HMC functional monomer.

Further, looking into the extent of interaction of the template with the crosslinkers, it is also possible that the divinyl benzene crosslinker would have higher binding affinity with the template, which would explain the large quenching effect observed when DVB was used crosslinker [28]. The competition that the crosslinker may offer with the functional monomer will not be favorable as it weakens the template-functional monomer interactions and therefore, the resulting MIP will demonstrate poor imprinting effect.

3.4.2. Effects of Varying Amounts of EGDMA on the Fluorescence of BAP-MIP

Establishing the utility of EGDMA in providing the necessary rigid yet porous MIP structure, subsequent formulations have utilized EGDMA as crosslinker. To further verify the amount of EGDMA

that will give the optimum fluorescent signal for MIP, different molar ratios of EGDMA were incorporated in the MIP formulation, i.e. 10, 20 and 30 mmoles. BAP was used as functional monomer in this case. In contrast to the observation with MIP-HMC, it was noted based from Fig. 7, that all MIPs-BAP gave relatively higher fluorescent intensities than the NIPs-BAP (no template added). In this case with BAP-MIP, instead of achieving fluorescent quenching, the presence of template molecules tends to enhance the fluorescence of BAP-MIP, with almost ~900 au. This observation was found to be consistent with the report of Kubo, *et al.* [16] that there was enhancement in the fluorescence signal of BAP upon binding with cyclobarbital. It is assumed that the increase in the fluorescence intensity could be due to the increase in rigidity of the MIP polymer network brought about by the incorporation of template molecules filling those pores or voids during polymerization.

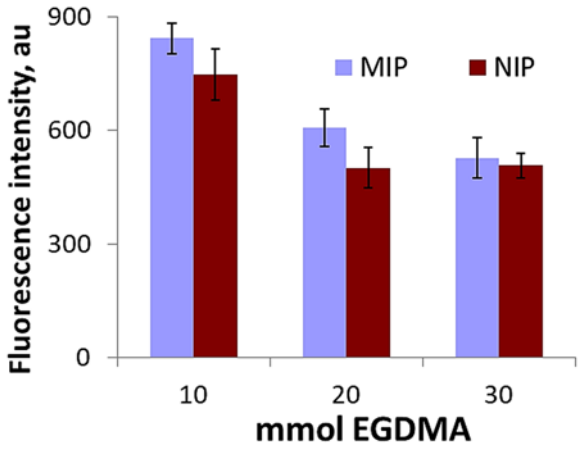

Fig. 7. Comparison of the fluorescent signals of MIPs and NIPs made from different molar ratios of EGDMA, with BAP as functional monomer.

Further into this experiment, both BAP-MIP and BAP-NIP prepared using a molar ratio of 1:4:10 (DNT:BAP:EGDMA) yielded the highest fluorescence intensities as compared to BAP-MIP samples prepared with EGDMA ratio 1:4:20 and 1:4:30 (DNT:BAP:EGDMA). The observed trend, in the order of decreasing emission intensities of BAP MIPs: 10 mmol EGDMA > 20 mmol EGDMA > 30 mmol EGDMA. It is rationalized that the relatively high fluorescent signal given by the 1:4:10 ratio can be attributed to inefficient polymerization. It could be that MIP structure contains some unpolymerized BAP monomers and template bound to unpolymerized BAP monomers in addition to template molecules entrapped within the MIP polymer network. Meanwhile, in the case of the 30 mmol EGDMA, the BAP-MIP structure could have become crosslinked due to favourable monomer-monomer interactions, leaving the polymer structure with limited number of template molecules. This would explain the almost the same intensities given by BAP-MIP and BAP-NIP, i.e. ~500 au. This is not favourable as this scenario could result to inefficient binding due limited number of binding sites for DNT. Also, the use of higher amount of crosslinker may not be cost-effective for practical purposes.

It is presuppose that considerable noncovalent interactions between BAP and DNT took place, with the fluorescent intensity of BAP-MIP containing 20 mmol EGDMA lower than what was achieved with 10 mmol EGDMA. The response of the BAP-MIP was sufficiently distinguishable compared to the two other responses. At this concentration of crosslinker, satisfactory crosslinking may have occurred, enough to provide stable polymeric support for the formation of binding sites arising from noncovalent DNT-BAP interactions. Therefore, it is assumed that the optimum amount to be used for EGDMA crosslinker was 20 mmol.

3.5. Surface Morphologies of MIPs

The surface characteristics of fluorescent MIPs were examined via Scanning Electron Microscopy (SEM). Fig. 8 displays the SEM images of BAP-MIPS prepared from different types of crosslinkers: a) TRIM; b) DVB and c) EGDMA. As shown, MIPs are comprised of highly porous structures particularly that of BAP-MIP prepared from EGDMA cross linker, typical of the surface profile of MIPs prepared via bulk polymerization. These porous structures are generally assumed to provide channels through which target analytes can access those imprint cavities. On the other hand, BAP-MIP prepared from DVB yielded quite different surface structure as there were no visible pores on the structure.

Meanwhile, surface morphologies of BAP-MIP prepared from varying molar ratios of EGDMA are shown in Fig. 9. SEM image shows the unique surface structures for each BAP-MIP prepared from different molar concentrations of EGDMA. MIP prepared from 20 mmol ratio gives porous surface but with more distinct features not visibly seen from the other BAP-MIPs.

The surface morphology of the BAP-MIP obtained from 10 mmol ratio of EGDMA correlates well with the observed fluorescence intensity. As illustrated, no unique porous-structure is demonstrated by the SEM image Fig. 9 (a). The rigidity in the polymer structure could explain why such MIP formulation yielded the highest fluorescence signal. On the other hand, MIP prepared from 30 mmol ratio of EGDMA gives a highly porous structure that could render the MIP less efficient in terms of providing support to the imprint cavities.

Fig. 10 are the SEM images of NIP prepared from a) HMC and b) BAP functional monomers.

Examining the SEM images reveal the completely different surface structure of NIP as compared to that of MIP. The difference is marked with the absence of any porous structures. In addition, rigidity in the structure is more pronounced in HMC-NIP compared to BAP-NIP.

In general, as shown by the SEM images of both MIP and NIP, it is evident that the surface structure is influenced by the: 1) Presence of target analyte during polymerization; 2) Type of crosslinker used; 3) Amount of crosslinker in the formulation.

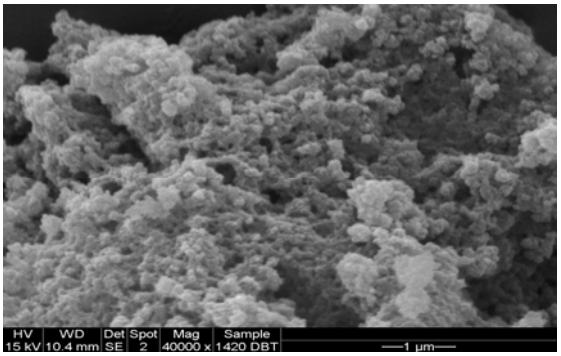

(a)

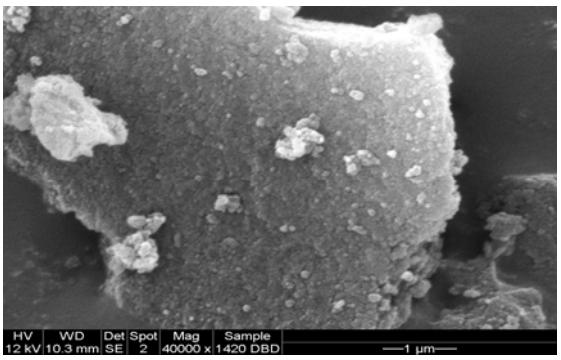

(b)

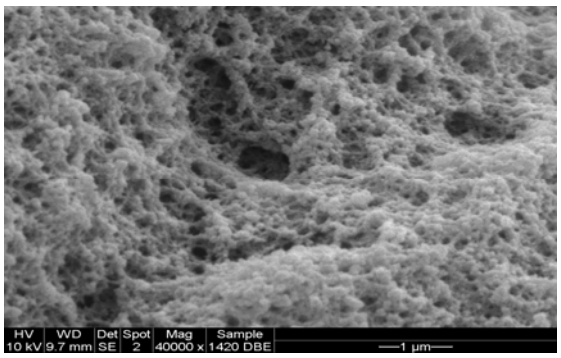

(c)

Fig. 8. SEM images of MIPs prepared from varying crosslinkers: DNT:BAP:X (1:4:20 molar ratio) where X: a) TRIM; b) DVB and c) EGDMA.

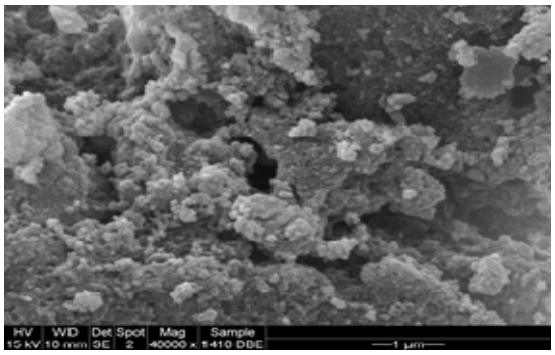

(a)

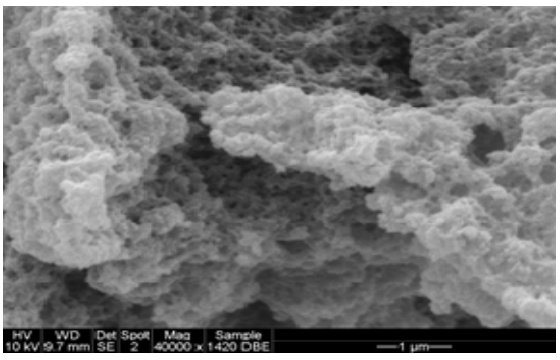

(b)

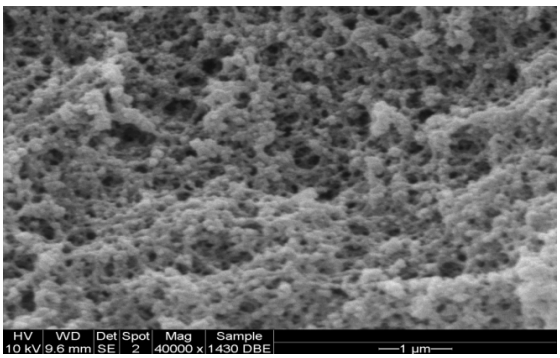

(c)

Fig. 9. Surface morphologies of MIPs prepared from varying molar ratios of DNT:BAP:EGDMA: a) 1:4:10; b) 1:4:20 and c) 1:4:30.

3.6. Incorporation of TNT in the MIP

In view of the findings obtained from the optimization steps, bulk/monolithic MIP polymers were individually prepared using 1:4:20 mmol ratio of template, monomer and EGDMA, with AIBN as initiator and DMF as porogen. NIPs were prepared using the same recipe but no template was added. FT-IR was used to confirm successful incorporation of template into the MIP network. As shown in Fig. 11, the highlighted area shows the TNT peak at about 1542 cm^{-1} which is due to the NO_2 asymmetric stretch. This peak did not appear in HMC-NIP.

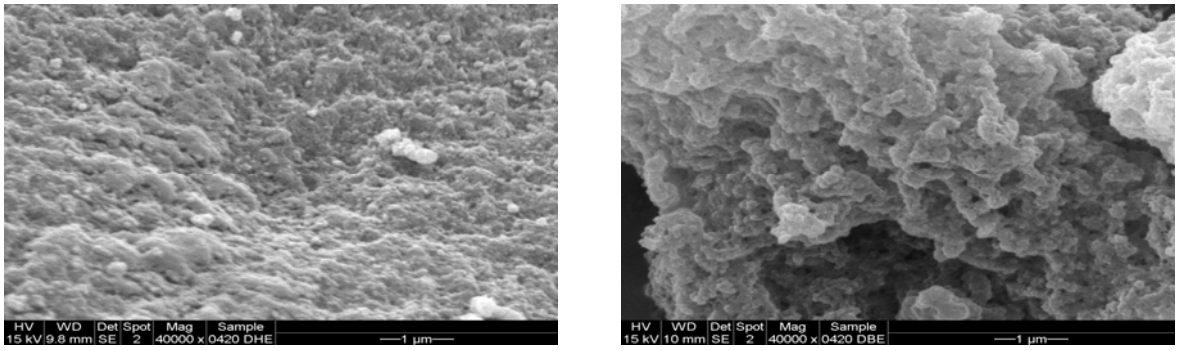

(a) (b)

Fig. 10. Surface morphologies of NIP prepared from: a) HMC and b) fluorescent BAP monomers.

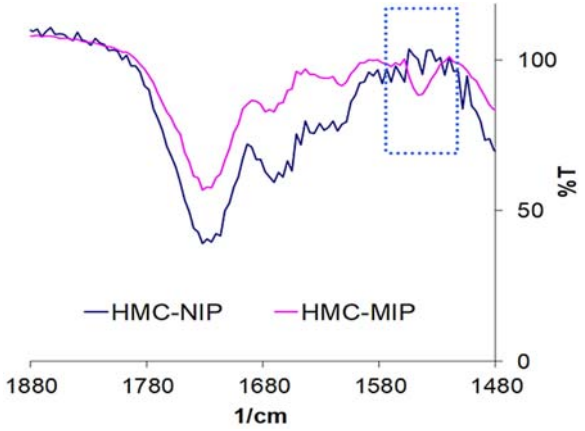

Fig. 11. FT-IR spectrum showing the successful incorporation of TNT molecules in the MIP structure.

Template removal in MIP was found to be effective via Soxhlet extraction using methanol:acetic acid solvent system, for 18 hours. NIPs were also subjected to same treatment to check on the influence of the solvent system on the overall MIP structure. However, it must be emphasized that the template molecules were not 100 % removed in MIP. Template removal was ascertained based from fluorescence measurements. Fluorescent signals of MIP and NIP before and after template removal were determined and compared.

3.7. Rebinding Experiments

The polymeric materials were ground and sieved to <38 μm and extracted (Soxhlet) to remove the template molecule. Each polymer was then re-exposed to varying concentrations of TNT and the fluorescence response was obtained by suspending 1 mg of the polymers in acetonitrile. Fig. 12 showed the fluorescence response of HMC-MIP and HMC-NIP in the presence of varying concentrations of TNT: 0 – 52 μM and 0 – 500 μM. As shown, the NIP (control) polymer response was found to be almost constant at concentration range 0 to 26 μM. On the other hand, fluorescence signal was found to decrease in the case of HMC-MIP, consistent with the earlier observation of quenching effect. Pronounced drop in the fluorescent signal, from 900 a.u. to ~500 a.u., was noted at TNT concentration less than 2.60 μM.

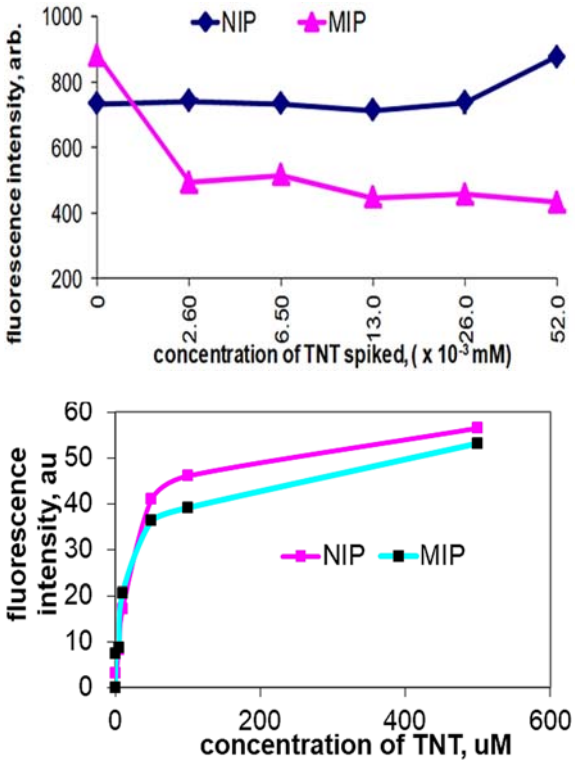

Fig. 12. Fluorescence response of MIP and NIP to varying concentrations of TNT: 0 – 52 μM (top) and 0 – 500 μM (below).

At higher concentration range, effective binding of TNT was found to occur starting from 50 μM to 500 μM. Moreover, it is also noted that in the presence of higher concentrations of TNT, HMC-MIP gave distinct response (quenching) toward the template as compared with the NIP (control polymer). This clearly demonstrates imprinting

effect; cavities were successfully created within the MIP network which then becomes binding sites for TNT in the MIP structure. In the case of NIP, since there was no template added in the recipe, it is taken up that there are no available binding sites formed and therefore any amount of TNT found to have bind with NIP can be treated as nonspecific binding only.

4. Conclusions

This study showcases the importance of tailoring the formulation for the preparation of fluorescent molecularly imprinted polymer. As shown, fluorescent monomer tends to interact uniquely with different target analytes. This observed difference in the template-functional monomer interactions is also manifested in the fluorescence response of the MIP upon binding with the template. HMC-MIP displayed fluorescence quenching effect whereas binding of template with BAP-MIP yield enhancement on the fluorescent signal. Further, template-functional monomer interaction may be studied using molecular modeling in tandem with NMR titration. This is to ensure that prior to polymerization, formation of binding sites are feasible as these template-monomer interactions shall dictate the success creation of binding sites within the MIP structure. In addition, it was also demonstrated that the type and amount of crosslinker can significantly alter the fluorescent signal of MIP. In this study, it was established that MIP formulation incorporating 20 mmol EGDMA yields MIP with obvious change in the fluorescence response. Such formulation exhibit the potential of detecting TNT in μM concentration range.

Acknowledgements

DCA gratefully acknowledges financial support from the Australian government through the Department of Education and Training's Endeavour Research Fellowship Award. The authors acknowledge support from the Australian Research Council and the University of Newcastle.

References

[1]. D. C. Apodaca, R. B. Pernites, R. R. Ponnapati, F. R. Del Mundo, R. C. Advincula, Electropolymerized Molecularly Imprinted Polymer Films of a Bis-terthiophene dendron: Folic Acid Quartz Crytal Microbalance Sensing, *ACS Appl. Mater. Interfaces*, Vol. 3, Issue 2, 2011, pp. 191-203.

[2]. R. Arshady, K. Mosbach, Synthesis of substrate-selective polymers by host-guest polymerization, *Macromolecular Chemistry and Physics*, Vol. 182, Issue 2, 1982, pp. 687-692.

[3]. S. Pradhan, M. Boopathi, O. Kumar, A. Baghel, P. Pandey, T. H. Mahato, B. Singh, R. Vijayaraghavan, Molecularly imprinted nanopatterns for the recognition of biological warfare agent ricin, *Biosens. Bioelectron*., Vol. 25, Issue 3, 2009, pp. 592-598.

[4]. S. Olsnes, The history of ricin, abrin and related toxins, *Toxicon.,* Vol. 44, Issue 4, 2004, pp. 361-370.

[5]. J. Audi, M. Belson, M. Patel, J. Schier, J. Osterloh, Ricin Poisoning, *JAMA,* Vol. 294, Issue 18, 2005, pp. 2342-2351.

[6]. M. V. Pishko, R. Stine, Comparison of glycosphingolipids and antibodies as receptor molecules for ricin detection, *Analytical Letters,* Vol. 77, Issue 9, 2005, pp. 2882-2888.

[7]. Ik-Bum Kim, J. N. Wilson, U. H. F. Bunz, Mannose-substituted PPES detect lectins: A model for ricin sensing, *Chem. Commun*., 2005, pp. 1273-1275.

[8]. S. M. Darby, M. Miller, R. Allen, Forensic determination of ricin and the alkaloid marker ricinine from Castor Bean extracts, *J. Forensic Science.,* Vol. 46, Issue 5, 2001, pp. 1033-1042.

[9]. R. C. Johnson, S. W. Lemire, A. R. Woolfitt, M. Ospina, K. P. Preston, C. T. Olson, J. R. Barr, Quantification of Ricinine in rat and human urine: A biomarker for ricin exposure, *J. Anal. Toxicol.,* Vol. 29, Issue 3, 2005, pp. 149-155.

[10]. A. C. Ferraz, M. E. M. Angelucci, M. L. Da Costa, I. R. Batista, B. H. De Oliveira, C. Da Cunha, Ricinine-elicited seizures: A novel chemical model of convulsive seizures, *Pharmacology Biochem. Behavior*, Vol. 65, Issue 4, 2000, pp. 577-583.

[11]. A. C. Ferraz, L. F. Pereira; R. L. Ribeiro, C. Wolfmar, J. H. Medina, F. A Scorza, N. F. Santos, E. A. Cavalheiro, Pharmacological evaluation of ricinine, a central Nervous system stimulant isolated from Ricinus communis, *Pharmacology Biochemistry and Behavior*, Vol. 63, Issue 3, 1999, pp. 367-375.

[12]. S. Chatterjee, U. Deb, S. Datta, C. Walther, D. K. Gupta, Common explosives (TNT, RDX, HMX) and their fate in the environment: Emphasizing bioremediation, *Chemosphere*, Vol. 184, 2017, pp. 438-451.

[13]. J. R. Wei, Y.-L. Ni, W. Zhang, Z.-Q. Zhang, J. Zhang, Detection of glycoprotein through fluorescent boronic acid-based molecularly imprinted polymers, *Analytica Chimica Acta*, Vol. 960, 201, pp. 110-116.

[14]. a) R. Wagner, W. Wan, M. Biyikal, E. Benito-Peña, M. C. Moreno-Bondi, I. Lazraq, K. Rurack, B. Sellergren, Synthesis, Spectroscopic and Analyte-Responsive Behavior of a Polymerizable Naphthalimide-based Carboxylate Probe and Molecularly Imprinted Polymers prepared thereof, *J. Org. Chem.,* Vol. 78, Issue 4, 2013, pp. 1377-1389; b) Z. Xu, P. Deng, S. P. Tang, J. Li, Fluorescent molecularly imprinted polymers based on 1,8-naphthalimide derivatives for efficiently recognition of cholic acid, *Mat. Sci. Eng. C*, Vol. 58, 2016, pp. 558-567.

[15]. Y. Inoue, A. Kuwahara, K. Ohmori, H. Sunayama, T. Ooya, T. Takeuchi, Fluorescent molecularly imprinted polymer thin films for specific protein detection prepared with dansyl ethylenediamine-conjugated O-acryloyl-L-hydroxyproline, *Biosens. Bioelectron*., Vol. 48, 2013, pp. 113-119.

[16]. H. Kubo, H. Nariai, T. Takeuchi, Multiple hydrogen bonding-based fluorescent imprinted polymers for cyclobarbital prepared with 2,6-bis(acryl)amidopyridine, *Chem. Commun*., 2003, pp. 2792-2793.

[17]. N. Thanh, D. C. Billington, N. A. Hartell, D. L. Rathbone, Selective recognition of cyclic GMP using a fluorescence-based molecularly imprinted polymer, *Analytical Letters,* Vol. 35, Issue 15, 2002, pp. 2499-2509.
[18]. A. Rachkov, S. McNiven, A. El'skaya, K. Yano, I. Karube, Fluorescence detection of beta-estradiol using a molecularly imprinted polymer, *Analytica Chimica Acta,* Vol. 405, Issue 1-2, 2000, pp. 23-29.
[19]. B. Wandelt, P. Turkewitsch, S. Wysocki, G. D. Darling, Fluorescent molecularly imprinted polymer studied by time-resolved fluorescence spectroscopy, *Polymer*., Vol. 43, 2002, pp. 2777-2785.
[20]. K. Dario, R. Olof, S. Anders, K. Mosbach, A Biomimetic Sensor based on a molecularly imprinted polymer as a recognition element combined with fiber optic detection, *Analytical Letters,* Vol. 67, Issue 13, 1995, pp. 2142-2144.
[21]. S. Kunath, N. Marchyk, K. Haupt, K-H Feller. Multiobjective optimization and design of experiments as tool to tailor molecular imprinted polymers specific for glucuronic acid. *Talanta*, Vol. 105, 2013, pp. 211-218.
[22]. D. R. Kryscio, N. A. Peppas. Critical review and perspective of macromolecularly imprinted polymers. *Acta Biomaterilia*, Vol. 8, 2012, pp. 461-473.
[23]. K. Yano, K. Tanabe, T. Takeuchi, J. Matsui, K. Ikebukuro, I. Karube, Molecularly imprinted polymers which mimic multiple hydrogen bonds between nucleotide bases, *Analytica Chimica Acta*, Vol. 363, Issue 2-3, 1998, pp. 111-117.
[24]. D. L. Rathbone, D. Su, Y. Wang, D. C. Billington, Molecular Recognition by Fluorescent imprinted polymers, *Tetrahedron Lett*., Vol. 41, Issue 1, 2000, pp. 123-126.
[25]. C. I. Holdsworth, M. C. Bowyer, C. Lennard, A. McCluskey, Formulation of cocaine-imprinted polymers utilizing molecular modeling and NMR analysis, *Aust. J. Chem.,* Vol. 58, Issue 5, 2005, pp. 315-320.
[26]. L. Schwarz, C. I. Holdsworth, A. McCluskey, M. C. Bowyer, Synthesis and evaluation of a molecularly imprinted polymer selective to 2,4,6-trichlorophenol, *Australian Journal of Chemistry*, Vol. 57, Issue 8, 2004, pp. 759-764.
[27]. F. Chu, G. Tsiminis, N. A. Spooner, T. M. Monro, Explosives detection by fluorescence quenching of conjugated polymers in suspended core optical fibers, *Sensors and Actuators B: Chemical*, Vol. 199, 2014, pp. 22-26.
[28]. T. Muhammad, Z. Nur, E. V. Piletska, O. Yimit, S. A. Piletsky, Rational design of molecularly imprinted polymers: The choice of cross-linker, *Analyst*, Vol. 137, Issue 11, 2012, pp. 2623-2628.
[29]. S. Shoravi, G. D. Olsson, B. C. G. Karlsson, I. A. Nicholls, On the influence of crosslinker on template complexation in molecularly imprinted polymers: A computational study of prepolymerization mixture events with correlations to template-polymer recognition behavior and NMR spectroscopic studies, *Int. J. Mol. Sci.,* Vol. 15, Issue 6, 2014, pp. 10622-10634.
[30]. H. Henschel, N. Kirsch, J. Hedin-Dahlstrom, M. J. Whitcombe, S. Wikman, I. A. Nicholls, Effect of the crosslinker on the general performance and temperature dependent behavior of a molecularly imprinted polymer catalyst of a Diels-Alder reaction, *Journal of Molecular Catalysis B*: *Enzymatic*, Vol. 72, Issue 3-4, 2011, pp. 199-205.
